PERGAMON

International Journal of Heat and Mass Transfer 44 (2001) 3463–3470

International Journal of HEAT and MASS TRANSFER

www.elsevier.com/locate/ijhmt

Convection in a square cavity filled with an anisotropic porous medium saturated with water near 4°C

W. Zheng, L. Robillard *, P. Vasseur

Department of Mechanical Engineering, Ecole Polytechnique, University of Montreal, CP 6079, Succ. Centre Ville, Montreal, Que., Canada H3C 3A7

Received 5 May 2000; received in revised form 27 November 2000

Abstract

A study is made of convection in an anisotropic porous medium saturated with water near 4°C, temperature at which the density reaches its maximum value. The saturated porous medium is contained in a square cavity with adiabatic horizontal walls and side walls subject to uniform temperatures. The parameters involved are the ratio of the extremum permeabilities K^*, the anisotropic angle θ giving the inclination of the principal axes, the Rayleigh number R and the inversion parameter γ, this last parameter being related to the horizontal position of the pure conduction 4°C isotherm relatively to the vertical walls. The problem is solved on the basis of the Darcy model and the Boussinesq approximation through the use of a finite difference numerical approach. For the case where the principal axes are parallel and perpendicular to the gravity vector, the Nusselt number is found to be maximum when the maximum permeability is in the vertical direction. For cases with oblique axes, no symmetric flow and temperature fields can be obtained at $\gamma = 1$ (pure conduction 4°C isotherm midway between the two side walls), as it is the case for an isotropic porous medium. Moreover, another difference with the isotropic case is the fact that the minimum Nusselt number does not occur at $\gamma = 1$ but at a value slightly different.

1. Introduction

Over the past years, a substantial part of theoretical and experimental investigations on convective heat transfer in porous media has dealt with the case of isotropic materials [1,2]. However, in many practical situations the porous materials are anisotropic in their mechanical as well as thermal properties. Most of the past studies on anisotropic porous media are concerned with the case of fluids having a linear relationship between density and temperature [3–8]. In general, the linear relationship is a good approximation for most practical applications.

Convection in cold water, however, behaves in a complicated manner when the temperature domain encompasses the 4°C, point at which the density of water reaches a maximum value. A few liquids, such as gallium, tellurium and molten bismuth, also possess a density extremum in their density temperature relationship. Convection in such fluids is referred to as an inversion density problem. Unusual flow patterns may be expected in areas of water exposed to near freezing temperature. The effect of inversion of density on heat transfer in different kinds of enclosures has been considerably investigated in the past. For instance, Watson [9], Seki et al. [10], Inaba and Fukuda [11,12], and, more recently, Ishikawa et al. [13] have considered the case of pure water confined in rectangular enclosures. Convection in isotropic porous media saturated with cold water and confined in rectangular cavities has been investigated first by Altimir [14]. Recently, transient natural convection of water near its density extremum, in a rectangular cavity filled with an isotropic porous medium, was investigated numerically by Chang and Yang [15]. The top and bottom walls were insulated and uniform temperatures were imposed on the left and right vertical walls, respectively. These authors showed that,

* Corresponding author. Tel.: +1-514-340-4711; fax: +1-514-340-5917.

E-mail address: robillard@meca.polymtl.ca (L. Robillard).

0017-9310/01/$ - see front matter
PII: S0017-9310(01)00004-7

Nomenclature

g	gravity acceleration (m s^{-2})
H'	height of the cavity (m)
k	saturated porous medium thermal conductivity (W m^{-1} K^{-1})
$\overline{\overline{K}}$	permeability tensor
K_1, K_2	permeability along the principal axes (m^2)
K^*	permeability ratio, $K^* = K_2/K_1$
Nu	overall Nusselt number, Eq. (13)
p'	pressure (N m^{-2})
R	Darcy Rayleigh number, $R = gK_2H'\lambda\Delta T'^2/\nu\alpha$
Rh	hydraulic resistivity, Eq. (14)
R_1	standard Darcy Rayleigh number, $R_1 = \lim_{\gamma\to\infty}(R_m\lvert\gamma\rvert)$
R_m	modified Rayleigh number, $R_m = 2R/(1+K^*)$
T	dimensionless temperature, $(T' - T'_R)/\Delta T'$
T'_R, T'_L	temperatures on right and left boundaries (°C)
T'_m	temperature of maximum density, 4°C
$\Delta T'$	characteristic temperature difference, $T'_L - T'_R$ (°C)
t	dimensionless time, $\sigma t'\alpha/H'^2$
u, v	dimensionless velocity components in x and y directions, $u'H'/\alpha$, $v'H'/\alpha$
x, y	dimensionless coordinate system, x'/H', y'/H'

Greek symbols

α	thermal diffusivity, $k/(\rho C)_f$ (m^2 s^{-1})
γ	inversion parameter, $\gamma = 2(T'_m - T'_R)/\Delta T'$
λ	thermal expansion coefficient (°C^{-2})
ν	kinematic viscosity of the fluid, m^2 s^{-1}
ρ	density of the fluid (kg m^{-3})
ρ_R	reference density (kg m^{-3})
$(\rho C)_f$	heat capacity of fluid (J m^{-3} s^{-1})
$(\rho C)_p$	heat capacity of saturated porous medium (J m^{-3} s^{-1})
ψ	dimensionless stream function, ψ'/α

for $\gamma < 1$, the size of the clockwise vortex beside the high-temperature surface increases as time increases. The clockwise vortex occupies almost the whole space when the steady state is reached. However, for $\gamma = 1$, two counter-rotating vortices having the same strength are observed in the cavity when steady state is reached. For $\gamma > 2$, only one counterclockwise vortex exists in the cavity.

Relatively little work has been done to study the effects of density inversion on the thermal convection within anisotropic porous media, in spite of their common occurrence in northern climates. The purpose of the present paper is aimed at a better understanding of such flows. We consider here the particular case of an anisotropic porous medium of square shape filled with water near its maximum density and subjected to side heating. The Darcy's flow model and a parabolic density temperature relationship are used.

2. Formulation of the problem

The physical system of interest is shown in Fig. 1. It consists of a square cavity of side H', filled with a water-saturated porous medium anisotropic in permeability. Horizontal boundaries are adiabatic. Vertical left and right boundaries are maintained at constant uniform temperatures T'_L and T'_R, respectively. Principal axes are shown with extremum permeabilities K_1 and K_2, the anisotropic angle θ giving the orientation of the principal axis labeled K_1 with respect to the horizontal x' axis.

The assumption of a Boussinesq incompressible fluid is adopted for water and physical properties other than the density in the buoyancy force are supposed constant. The density is assumed to vary with temperature according to a parabolic relationship of the form

$$\frac{\rho - \rho_m}{\rho_R} \approx \frac{\rho - \rho_m}{\rho_m} = -\lambda(T' - T'_m)^2, \tag{1}$$

where ρ_R is a reference density. With $T'_m = 3.98$°C and $\lambda = 8.0 \times 10^{-6}$ (°C)$^{-2}$ for water, the resulting equation is valid for the range 0–8°C [16]. A relationship of higher order (see for instance [17]) is not required since all the essential features characterizing convection with a density extremum are reproduced with the simple form of Eq. (1). An exhaustive view of the problem is then possible with the addition of a single parameter, the inversion parameter, to be defined later.

The continuity, momentum and energy conservation equations that govern the flow and heat transfer inside the enclosure are:

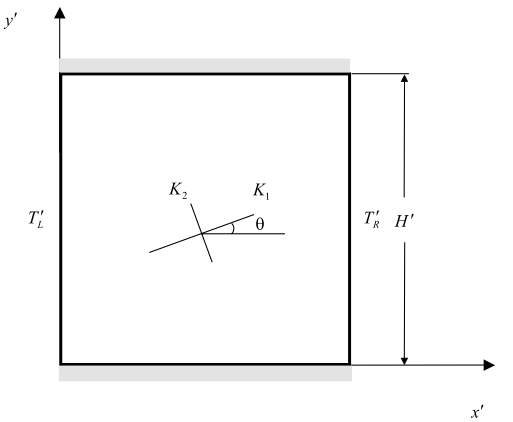

Fig. 1. Definition of the problem.

$$\nabla \cdot \vec{V}' = 0, \tag{2}$$

$$\vec{V}' = \frac{\overline{\overline{K'}}}{\mu}(-\nabla p' + \Delta\rho\vec{g}), \tag{3}$$

$$\sigma\frac{\partial T'}{\partial t'} + \vec{V}' \cdot \nabla T' = \alpha\nabla^2 T'. \tag{4}$$

In the above equation, $\overline{\overline{K'}}$ is the second-order permeability tensor, $\vec{V}'$ the mass averaged velocity, $\vec{g}$ the gravity vector, $\alpha = k/(\rho_R C)_f$ the thermal diffusivity, and $\sigma = (\rho_R C)_p/(\rho_R C)_f$ the heat capacity ratio.

From Eq. (1) it follows that the density difference involved in Eq. (3) may be expressed as

$$\begin{aligned}\Delta\rho &= (\rho - \rho_m) - (\rho_R - \rho_m)\\ &= \rho_m\lambda[2(T'_m - T'_R)(T' - T'_R) - (T' - T'_R)^2].\end{aligned} \tag{5}$$

The unknown variables of the present problem are the velocity components (u', v'), pressure p' and temperature T'. It is convenient to introduce the stream function ψ' defined as

$$u' = \frac{\partial\psi'}{\partial y'}, \quad v' = -\frac{\partial\psi'}{\partial x'}. \tag{6}$$

Such a definition of u' and v' automatically satisfies the continuity equation (2). Using H', α, α/H' and $\Delta T' = T'_L - T'_R$ as respective scales for length, stream function, velocity and temperature, and taking the curl of the momentum equation leads to the following dimensionless equations:

$$a\frac{\partial^2\psi}{\partial x^2} + b\frac{\partial^2\psi}{\partial x\partial y} + c\frac{\partial^2\psi}{\partial y^2} = R(\gamma - 2T)\frac{\partial T}{\partial x}, \tag{7}$$

$$\frac{\partial T}{\partial t} + u\frac{\partial T}{\partial x} + v\frac{\partial T}{\partial y} = \frac{\partial^2 T}{\partial x^2} + \frac{\partial^2 T}{\partial y^2}, \tag{8}$$

where

$$\begin{aligned}a &= \cos^2\theta + K^*\sin^2\theta,\\ b &= (1 - K^*)\sin 2\theta,\\ c &= K^*\cos^2\theta + \sin^2\theta.\end{aligned} \tag{9}$$

In the above equations, $R = gK_2H'\lambda\Delta T'^2/(v\alpha)$ is the Darcy Rayleigh number and $K^* = K_2/K_1$ is the permeability ratio. The dimensionless temperature is defined as $T = (T' - T'_R)/\Delta T'$. The parameter γ, defined as

$$\gamma = 2\frac{T'_m - T'_R}{\Delta T'}, \tag{10}$$

is called the inversion parameter. It determines, in pure conduction, the position of T'_m with respect to the two vertical boundaries. The standard case of linear convection is recovered when $\gamma \to \infty$, with $R_l = \lim_{\gamma\to\pm\infty}(|\gamma|R)$, R_l being the standard form of the Darcy Rayleigh number used when ρ is linearly related to T.

The governing parameters in the present problem are the Rayleigh number R, the inversion parameter γ, the permeability ratio $K^* = K_2/K_1$ and the anisotropic angle θ.

Hydrodynamic boundary conditions on all solid boundaries are

$$\psi = 0 \tag{11}$$

while the thermal boundary conditions are given by

$$\begin{aligned}x = 0, 1: &\quad T = 1, 0,\\ y = 0, 1: &\quad \frac{\partial T}{\partial y} = 0.\end{aligned} \tag{12}$$

The rate of heat transfer is given by the overall Nusselt number evaluated on the left or right boundaries and defined as

$$Nu = \int_0^1 \left.\frac{\partial T}{\partial x}\right|_{x=0,1} dy. \tag{13}$$

In order to isolate the effect of a change in permeability ratio K^* from the change in the overall hydraulic resistivity (the hydraulic resistivity being the inverse of the permeability [18]) it is appropriate to define a new Rayleigh number. By considering the two hydraulic resistivities along the principal axes, $Rh_1 = 1/K_1$ and $Rh_1 = 1/K_1$, we define an overall hydraulic resistivity $\overline{Rh}$ as

$$\overline{Rh} = \frac{Rh_1 + Rh_2}{2} = \frac{1}{2}\frac{K_1 + K_2}{K_1K_2} \tag{14}$$

and a modified Rayleigh number as

$$R_m = \frac{g\lambda\Delta T^2 H}{v\alpha}\frac{1}{\overline{Rh}} = \frac{2R}{1 + K^*} \tag{15}$$

with the consequence that the extremum permeabilities K_1 and K_2 have the same weight in this new Rayleigh number.

3. Numerical approach

Governing Eqs. (7) and (8) with boundary conditions (11) and (12) were solved with a finite difference approach. The entire domain shown in Fig. 1 was discretized with a uniform mesh size. Eq. (7) was solved by the method of successive over-relaxation and alternative direction implicit (ADI) method was used to solve Eq. (8). The advective terms were formulated by central differences.

For the limiting case of an isotropic porous medium ($K^* = 1$), a comparison of overall Nusselt numbers with those obtained by Ni and Beckermann [3] is presented in Table 1. It can be seen that the present Nusselt numbers fall within 2% of the calculations of Ni and Beckermann.

The present numerical procedure was also tested for the linear range density–temperature by comparison with Nusselt numbers obtained by Degan and Vasseur

Table 1
Comparison with the results of Ni and Beckermann [3]

Rayleigh number	Ni	Present
100	3.103	3.124
500	8.892	9.000
1000	13.420	13.413

[7] for various Rayleigh numbers R_l, permeability ratios K^* and anisotropic angles θ (see Table 2). Flow and temperature fields shown in [7] were also reproduced with satisfying accuracy.

The effect of mesh size on the numerical simulation was tested before the new method was applied to the research. The case G in Table 2 was used to perform the mesh size independent test. It was found with increasing mesh size from 80×80 to 100×100, that less than 0.009% difference would happen between two Nusselt numbers (see Table 3). So, 80×80 were used in most of our research. Moreover, in order to keep all of the results independent of mesh size, a careful verification test was done for each case.

Table 3
Mesh size independent test

Mesh size	40×40	60×60	80×80	100×100
Nusselt number	4.3489	4.3700	4.3729	4.3733

4. Results and discussion

As described by many authors (see for instance [19]) the effect of density inversion on the convection of cold water, confined in an enclosure, is to give rise to a multicellular flow pattern, thus reducing the heat transfer through the cavity. This statement remains true for the present problem, as it will be illustrated by the following results. In the present part, in addition to the effect of the Rayleigh number R_m, we will discuss in order the separate effects of the inversion parameter γ, of the permeability ratio K^*, of the anisotropic angle θ and finally of the combined effects of θ and γ.

4.1. Effect of the inversion parameter γ (isotropic case $K^* = 1$)

For the case of a square cavity such as the one considered in the present study, the relative position, $x_m = 1 - \gamma/2$, of the pure conduction 4°C isotherm with respect to the two vertical boundaries will strongly influence the convective heat transfer and the associated flow field. The numerical results (not presented here) indicated that with γ increasing toward large values, the standard case of convection with linear density temperature relationship is recovered. When $\gamma = 1$, a symmetric flow is obtained. Such a behavior has already been observed by many authors (see for instance [20–22]).

The Nusselt number reaches its minimum value at $\gamma = 1$, as already found by Lin and Nansteel [22] and the following relationship holds:

$$Nu(\gamma) = Nu(2 - \gamma) \tag{16}$$

with corresponding flow fields being mirror images.

4.2. Effect of the permeability ratio K^* ($\gamma = 1, \theta = 0$)

As reported in the literature [20–22], a symmetric flow field with two counter-rotating convective cells is obtained for $\gamma = 1$ and $K^* = 1$. This symmetry at $\gamma = 1$ remains for the anisotropic case with $\theta = 0°$ and 90°.

Fig. 2 shows the Nusselt number Nu, defined in Eq. (13), function of the permeability ratio K^* for different Rayleigh numbers R_m (200, 400, 600 and 800), the anisotropic angle θ being maintained at 0. Owing to the definition of R_m, the overall hydraulic resistivity remains constant along each curve of Fig. 2. From the behavior of the curves in this figure, it is clear that a relative increase of the vertical permeability will enhance the heat transfer in the horizontal direction.

The effect of K^* on the flow and temperature fields is shown in Fig. 3(a)–(d), for $R_m = 400$, $\gamma = 1$ and $\theta = 0°$.

Table 2
Comparison with the results of Degan and Vasseur [7]

Case	Rayleigh number, R_l	Permeability ratio, K^*	Anisotropic angle, θ	Mesh size, $x \times y$	Present method, Nu	Degan and Vasseur [7], Nu
A	400	0.01	45°	100×120	11.483	11.313
B	400	1	45°	80×80	7.884	7.859
C	400	100	45°	80×80	1.090	1.090
D	1	0.001	0°	80×80	1.004	1.003
E	1	0.001	90°	80×80	1.004	1.003
F	10,000	100	0°	100×120	9.741	9.967
G	10,000	100	90°	80×80	4.373	4.341

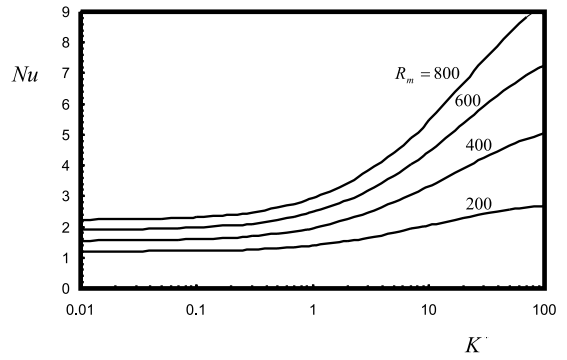

Fig. 2. Nusselt number function of permeability ratio K^* and R_m ($\theta = 0°$, $\gamma = 1$).

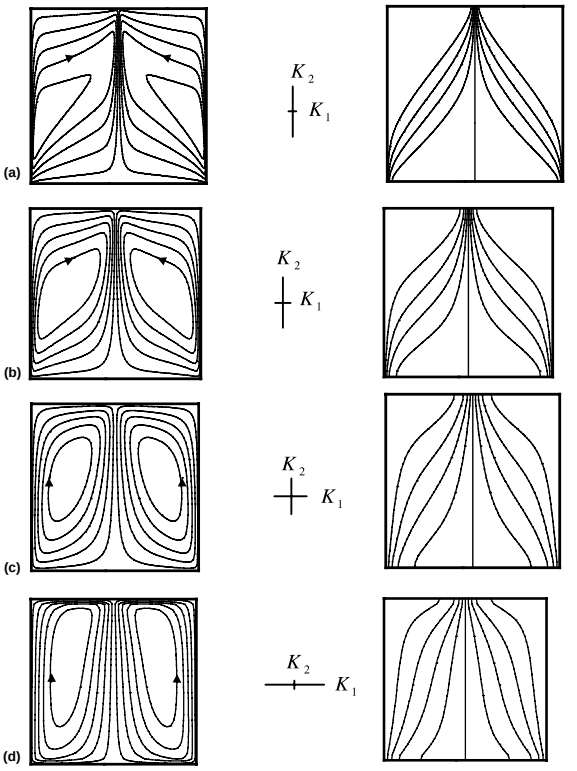

Fig. 3. Flow and temperature fields at various K^* ($\gamma = 1$, $R_m = 400$, $\theta = 0°$): (a) $\psi_{max} = 13.77$, $\psi_{min} = -13.77$, $K^* = 100$, $Nu = 5.07$; (b) $\psi_{max} = 8.68$, $\psi_{min} = -8.68$, $K^* = 10$, $Nu = 3.33$; (c) $\psi_{max} = 4.89$, $\psi_{min} = -4.89$, $K^* = 1$, $Nu = 1.97$; (d) $\psi_{max} = 3.16$, $\psi_{min} = -3.16$, $K^* = 0.01$, $Nu = 1.55$.

It is seen that the distortion of the isotherms is reduced with K^* decreasing, the amount of distortion being related to the importance of the convective heat transfer. However, for each of the flow and temperature fields shown in Fig. 3, the symmetry with respect to a vertical line separating the cavity in two halves is preserved.

4.3. Effect of the anisotropic angle θ

Figs. 4 and 5 give the Nusselt number, Nu, and the extremum values of the stream function, ψ_{max} and ψ_{min}, as functions of the orientation angle θ. The extremum values ψ_{max} and ψ_{min} respresent the intensities of the right and left convective cells, respectively. In both Figs. 4 and 5, three sets of curves are shown, corresponding to modified Rayleigh numbers R_m of 200, 400 and 800. For all those curves, γ and K^* are kept constant at respective values of 1 and 0.1. Flow and temperature fields corresponding to $R_m = 800$ are shown in Fig. 6(a)–(e) for different values of θ from 0° to 90°. We may observe in Fig. 4 the continuous transition for Nu, from its minimum value to its maximum value, with θ increasing from 0° to 90°, i.e., when the maximum permeability axis is tilted from the horizontal to the vertical direction. In Fig. 5, $|\psi_{min}|$ and ψ_{max} are seen to evolve from the value $|\psi_{min}| = \psi_{max} = 6.03$ at $\theta = 0°$ to the value $|\psi_{min}| = \psi_{max} = 14.61$ at $\theta = 90°$. This equal intensity of the two counterrotating cells at 0° and 90° is related to the symmetry described previously for the isotropic case and the anisotropic case with $\theta = 0°$C.

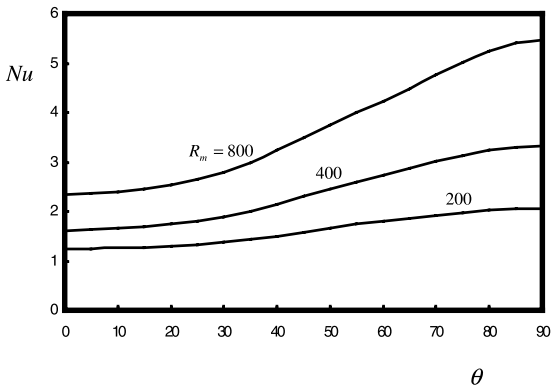

Fig. 4. Nusselt number function of θ ($\gamma = 1$, $K^* = 0.1$).

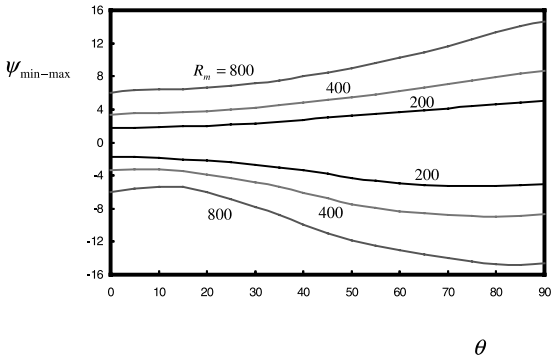

Fig. 5. Extremum values ψ_{max} and ψ_{min} function of θ ($\gamma = 1$, $K^* = 0.1$).

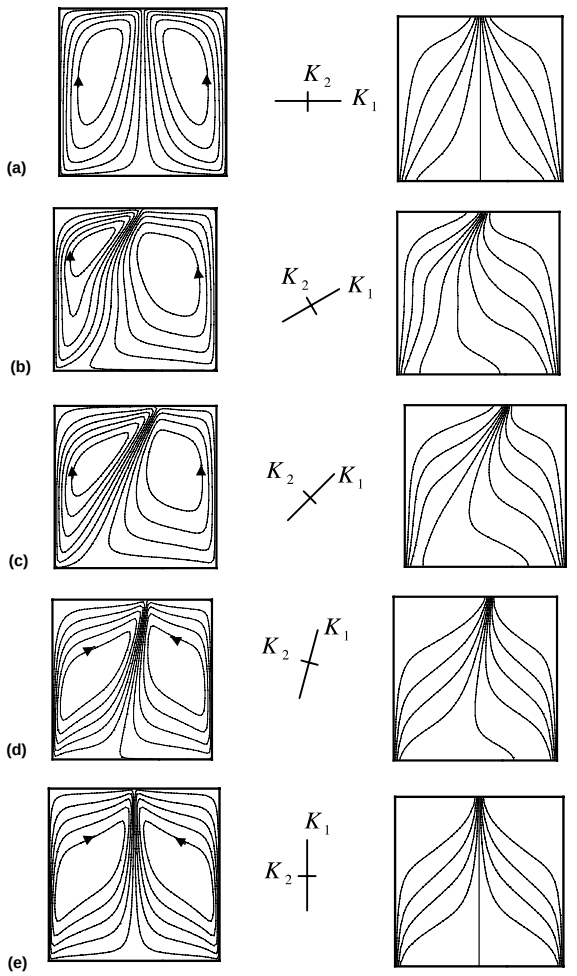

Fig. 6. Flow and temperature fields at various θ ($R_m = 800$, $\gamma = 1$, $K^* = 0.1$): (a) $\theta = 0°$, $\psi_{max} = 6.03$, $\psi_{min} = -6.03$, $Nu = 2.33$; (b) $\theta = 35°$, $\psi_{max} = 7.12$, $\psi_{min} = -7.77$, $Nu = 2.74$; (c) $\theta = 45°$, $\psi_{max} = 8.50$, $\psi_{min} = -11.01$, $Nu = 3.45$; (d) $\theta = 75°$, $\psi_{max} = 12.46$, $\psi_{min} = -14.43$, $Nu = 5.00$; (e) $\theta = 90°$, $\psi_{max} = 14.61$, $\psi_{min} = -14.61$, $Nu = 5.47$.

However, for $0° < \theta < 90°$, this symmetry does not exist, as it can be observed in the sequence of flow and temperature fields of Fig. 6. With θ increasing from 0° to 90°, $|\psi_{min}|$ decreases at first to reach a minimum value of about 5.5 at $\theta \approx 13°$, for the case $R_m = 800$, whereas ψ_{max} increases continuously from 0° to 90°. Beyond $\theta \approx 13°$, $|\psi_{min}|$ starts increasing faster than ψ_{max} and $|\psi_{min}| = \psi_{max}$ at $\theta \approx 24°$.

The following trivial periodicity holds for an anisotropic porous medium:

$$\psi(\theta) = \psi(\theta \pm n\pi), \quad T(\theta) = T(\theta \pm n\pi), \tag{17}$$

where $n = 1, 2, \ldots$ Moreover, at $\gamma = 1$, the left and right cell intensities are related according to

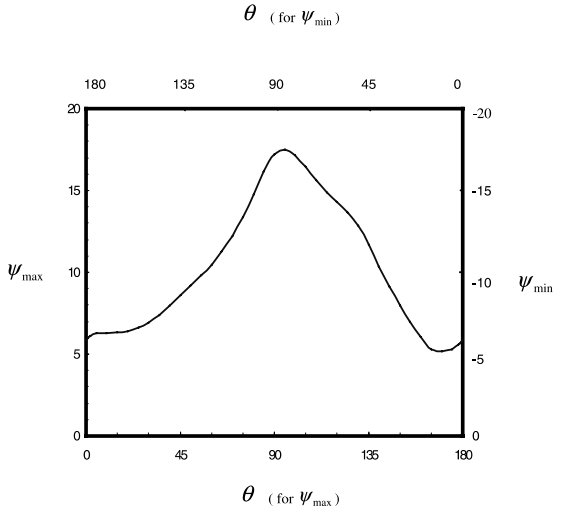

Fig. 7. Extremum values ψ_{max} and ψ_{min} function of θ ($R_m = 800$, $\gamma = 1$, $K^* = 0.05$).

$$\psi_{max}(\theta) = -\psi_{min}(\pi - \theta). \tag{18}$$

From Eq. (18), it is therefore possible to represent ψ_{min} and ψ_{max} as functions of θ, on a single curve such as the one given in Fig. 7. One may notice in this figure that the maximum value ψ_{max} (or $|\psi_{min}|$) occurs when the maximum permeability axis is titled at an angle of about 5° off with respect to the vertical direction (90°) and that the minimum value ψ_{max} (or $|\psi_{min}|$) occurs when the maximum permeability axis is titled at an angle of about 9° off with respect to the horizontal direction.

4.4. Combined effect of γ and θ

It has been mentioned that the Nusselt number reaches its minimum value at $\gamma = 1$ and the results are symmetric according to Eq. (16), for an isotropic porous medium. That symmetry was already observed by Lin and Nansteel [22]. Moreover, at $\gamma = 1$ flow and temperature fields are found to be symmetric with respect to a vertical line separating the whole cavity in two equal parts. This last symmetry of the flow and temperature fields holds for $K^* \neq 1$ (anisotropic medium) provided that $\theta = 0°$ or 90°. Fig. 8 shows the combined effect of γ and θ on the Nusselt number. In this figure, the Rayleigh number R_m and the permeability ratio K^* have the respective values 100 and 0.05. It is clear from this figure that the symmetry of the curves with respect to $\gamma = 1$ does not exist anymore for the anisotropic medium with oblique principal axes.

For the isotropic porous medium and also for the anisotropic case with $\theta = 0°$ or 90° the minimum Nusselt number at $\gamma = 1$ corresponds to a symmetric flow field, the anisotropic case being shown in Fig. 6(a) and (e),

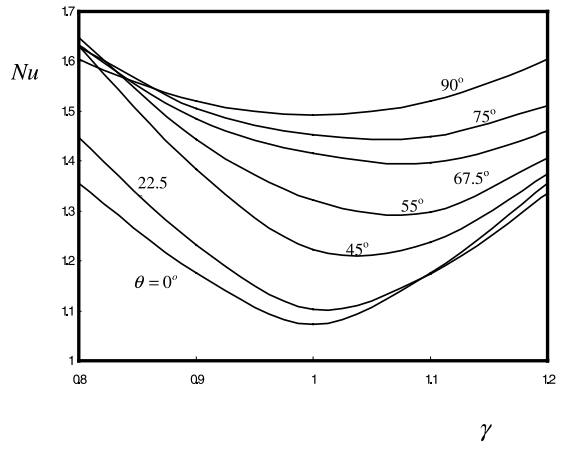

Fig. 8. Nusselt number function of γ at various θ ($R_m = 100$, $K^* = 0.05$).

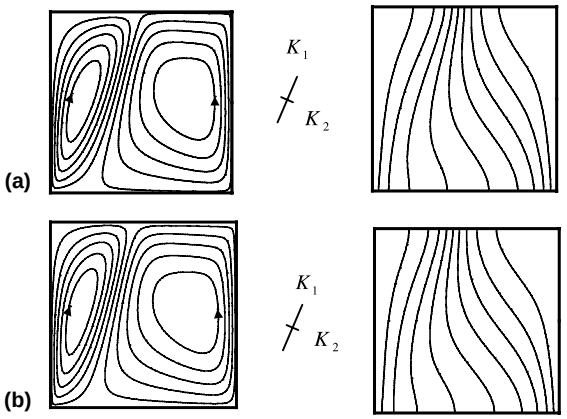

Fig. 9. Flow and temperature fields at $\theta = 67.5°$ ($R_m = 100$, $K^* = 0.05$): (a) $\psi_{max} = 2.545$, $\psi_{min} = -2.855$, $Nu = 1.3954$, $\gamma = 1.09$; (b) $\psi_{max} = 2.573$, $\psi_{min} = -2.564$, $Nu = 1.4002$, $\gamma = 1.12$.

with $|\psi_{min}| = \psi_{max}$. Such a symmetry at minimum Nu does not exist anymore when $\theta \neq 0°$ or 90° for an anisotropic porous medium. For instance, Fig. 9(a) and (b) shows the flow and temperature fields for $K^* = 0.05$, $R_m = 100$, $\theta = 67.5°$, at two different values of γ. Fig. 9(a), corresponds to the minimum value of Nu, obtained at $\gamma = 1.09$ (see Fig. 8), with $|\psi_{min}| = 2.86$ and $\psi_{max} = 2.55$. Fig. 9(b) obtained at $\gamma = 1.12$ shows two cells with equal intensity $|\psi_{min}| = \psi_{max} \approx 2.56$, but without symmetric flow field.

5. Conclusions

The effects of density inversion characterizing water near 4°C have been investigated for the case of an anisotropic porous medium, saturated with water, contained in a square cavity, the two vertical side walls being maintained at uniform temperatures. Numerical results were obtained for various anisotropic angles θ, permeability ratios K^* and values of the inversion parameter γ, this last parameter being directly related to the horizontal position of the pure conduction maximum density with respect to the side walls.

Results with $\theta = 0°$ and 90° (horizontal/vertical principal axes) indicate that the maximum convection and heat transfer occur when the maximum permeability is in the vertical direction. With oblique axes ($\theta \neq 0°$ or 90°), it was found that the symmetry of flow and temperature fields observed for the isotropic porous medium at $\gamma = 1$ (value for which the temperatures of the side walls are equidistant from the maximum density temperature of 4°C) does not exist anymore for the anisotropic porous medium. Moreover, for those conditions, the minimum Nusselt number does not occur at $\gamma = 1$, but is shifted slightly above or below unity, at a value for which the symmetry of flow and temperature field is not recovered.

Acknowledgements

Financial support by Natural Sciences and Engineering Concil of Canada and by FCAR from Province of Quebec are acknowledged.

References

[1] D.A. Nield, A. Bejan, in: Convection in Porous Media, Springer, New York, 1992.
[2] D.B. Ingham, I. Pop, in: Transport Phenomena in Porous Media, Pergamon, Oxford, 1998.
[3] J. Ni, C. Beckermann, Natural convection in a vertical enclosure filled with anisotropic porous media, Trans. ASME: J. Heat Transfer 113 (1991) 1033–1037.
[4] R. Mckibbin, P.A. Tyvand, Anisotropic modelling of thermal convection in multi-layered porous media, J. Fluid Mech. 118 (1982) 315–339.
[5] T. Nilsen, L. Storesletten, An analytical study on natural convection in isotropic and anisotropic porous channels, Trans ASME: J. Heat Transfer 112 (1990) 396–401.
[6] M. Trew, R. Mckibbin, Convection in anisotropic inclined porous layers, Transp. Porous Media 17 (1994) 271–283.
[7] G. Degan, P. Vasseur, Natural convection in a vertical slot filled with an anisotropic porous medium with oblique principal axes, Numer. Heat Transfer A 30 (1996) 397–412.
[8] P. Bera, V. Eswaran, P. Singh, Numerical study of heat and mass transfer in an anisotropic porous enclosure due to constant heating and cooling, Numer. Heat Transfer A 34 (1998) 887–905.
[9] A. Watson, The effect of the inversion temperature on the convection of water in an enclosed rectangular cavity, Quart. J. Mech. Appl. Math. 25 (4) (1972) 423–446.

[10] N. Seki, S. Fukusako, H. Inaba, Sapporo, Free convective heat transfer with density inversion in a confined rectangular vessel, Warme Stoffubertrag. 11 (1978) 145–156.
[11] H. Inaba, T. Fukuda, Natural convection in an inclined square cavity in regions of density inversion of water, J. Fluid Mech. 142 (1983) 363–381.
[12] H. Inaba, T. Fukuda, An experimental study of natural convection in an inclined rectangular cavity filled with water at its density extremum, J. Heat Transfer 106 (1984) 109–115.
[13] M. Ishikawa, T. Hirata, S. Noda, Numerical simulation of natural convection with density inversion in a square cavity, Numer. Heat Transfer A 37 (2000) 395–406.
[14] I. Altimir, Three-dimensional free heat transfer in saturated porous media with maximum density effects, Int. J. Heat Mass Transfer 27 (1984) 1813–1824.
[15] W.J. Chang, D.F. Yang, Transient natural convection of water near its density extremum in a rectangular cavity filled with porous medium, Numer. Heat Transfer A 28 (1995) 619–633.
[16] D.R. Moore, N.O. Weiss, Nonlinear penetrative convection, J. Fluid Mech. 61 (1973) 553–581.
[17] M. Mamou, L. Robillard, P. Vasseur, Thermoconvective instability in a horizontal porous cavity saturated with cold water, Int. J. Heat Mass Transfer 42 (1999) 4487–4500.
[18] J. Bear, in: Dynamics of Fluids in Porous Media, Dover, New York, 1988.
[19] L. Robillard, P. Vasseur, Convective flow generated by a pipe in a semi-infinite porous medium saturated with water in the neighburhood of 4°C, in: K.C. Chang, N. Seki (Eds.), in: Freezing and Melting Heat Transfer in Engineering, Hemisphere, Washington, DC, 1991, pp. 315–338.
[20] L. Robillard, P. Vasseur, Effet du maximum de densité sur la convection libre de l'eau dans une cavité fermée, Can. J. Civil Eng. 6 (1979) 481–493.
[21] W. Tong, J.N. Koster, Density inversion effect on transient natural convection in a rectangular enclosure, Int. J. Heat Mass Transfer 37 (1994) 927–938.
[22] D.S. Lin, M.W. Nansteel, Natural convection heat transfer in a square enclosure containing water near its density extremum, Int. J. Heat Mass Transfer 30 (1987) 2319–2329.